

Relativistic All-Electron Density Functional Calculations

CHRISTOPH VAN WÜLLEN

Lehrstuhl für Theoretische Chemie, Fakultät für Chemie, Ruhr-Universität, D-44780 Bochum, Germany

Received 8 June 1998; accepted 18 August 1998

ABSTRACT: The current status of relativistic density functional theory is reviewed. For most applications relevant to chemistry, relativistic corrections to the electron interaction and radiative corrections are not important, and the (four-component) Dirac–Kohn–Sham model can be viewed as a reference. More approximate (two-component) schemes are much more popular not only because of the lower computational effort, but also because, in chemistry, one is only interested in the electronic states of a system, and the two-component methods in one way or another project out the positronic states. It is even possible to arrive at one-component relativistic methods if one can neglect spin-orbit coupling, which is often done for closed-shell compounds containing heavy atoms. Various such schemes are available today, based on first-order perturbation theory or even including higher order corrections, based on the Douglas–Kroll–Hess transformation, or on the so-called regular approximation. In recent years, analytical geometry gradients have been implemented for all these methods, the gradient for the zeroth-order regular approximation (ZORA) being presented in this work for the first time. The availability of such geometry gradients is quite important for the applicability of these methods to “real chemistry”; that is, polyatomic molecules. Results of relativistic density functional methods are collected for some benchmark molecules. Then some results for various tungsten pentacarbonyl phosphines, platinum tricarbonyl phosphines, and molybdenum dinitrogen phosphine carbonyls, as obtained with first-order relativistic density functional calculations by means of direct perturbation theory (DPT), are presented. In another application, the force field of molybdenum, tungsten, and uranium hexafluoride in the metal–fluorine stretch region is calculated at both the DPT and ZORA levels. First-order relativistic calculations are reasonable for second- and third-row transition metal compounds (mainly 4d and 5d electrons involved in bonding), whereas, for uranium and gold compounds (mainly 5f, 6d, and 6s electrons involved), higher order relativistic corrections must be considered. © 1999 John Wiley & Sons, Inc. *J Comput Chem* 20: 51–62, 1999

Correspondence to: C. van Wüllen

Introduction

The most famous words of Paul Dirac are probably in his statement indicating that the whole of chemistry lies in the Schrödinger equation (first paragraph of ref. 1). This statement is erroneous, not only because the idea of reducing chemistry to physics is highly problematic,² but also because Dirac arrived at his conclusion after explicitly assuming that electrons in atoms and molecules are low-energy particles for which effects associated with special relativity are irrelevant. Since the early 1970s it became more and more widely appreciated that this is not the case. In heavy atoms (with high nuclear charge), the magnitude of the kinetic energy of the core electrons leads to a contraction and stabilization of s- and p-type orbitals (in both the core and valence shells). A better electrostatic shielding of the nucleus results, which in turn causes an expansion and destabilization of d- and f-type orbitals. The bonding in transition metal compounds, for example, is sensitive to the $nd - (n + 1)s$ energy gap ($n = 3, 4, 5$ for first-, second-, and third-row transition metals, respectively), and nonrelativistic calculations are not even qualitatively correct for third-row transition metal compounds. It should be noted that relativistic effects can also be important in compounds that contain only light atoms. The symmetry of the nonrelativistic Hamiltonian is broken by spin-orbit coupling, and this allows singlet-triplet transition, which has great importance in, for example, organic photochemistry. For reviews about relativistic effects in heavy-element chemistry, the reader is referred to refs. 3 and 4.

Having seen that relativistic effects play an important role in chemistry, we now review how relativity can be incorporated into density functional theory, and report the progress that has been achieved in recent years. Today, a variety of relativistic all-electron density functional methods are available, and analytical geometry gradients have been formulated and implemented for all relevant methods quite recently. The contributions of the present investigator to this development include gradients for relativistic direct perturbation theory and for zeroth-order regular approximation, the latter being presented here for the first time.

Finally, one should not forget that many density functional calculations performed today include

relativity, mostly at the scalar-relativistic level, through the use of relativistic effective core potentials (for a recent application, see ref. 5). Such calculations are beyond the scope of this report and will not be considered further.

Dirac-Kohn-Sham Model, Two- and One-Component Schemes

The wave equation for a noninteracting relativistic electron is the well-known Dirac equation. It describes correctly the relativistic kinematics of an electron, its spin, and the coupling of the electron spin to its linear momentum. In atoms and molecules, we have to consider that nuclei and electrons are charged and thus interact, the interaction being mediated by the electromagnetic field. This leads to relativistic corrections to the electron interaction itself, and to other relativistic effects like vacuum polarization and self-energy ("Lamb shift"), etc.

Relativistic corrections to the electron interaction are not known in closed form. In quantum-chemical calculations, one rarely goes beyond the leading order correction (the Breit term⁶), which includes the retardation of the Coulomb potential and magnetic interactions. Corrections to the Dirac equation, such as the Lamb shift, are considered only on occasion,⁷ although they are of similar importance in the valence shell. Experience gained so far indicates that valence properties of atoms and molecules (e.g., first to fourth ionization potentials, bond lengths, binding energies, etc.) are hardly affected by the relativistic correction to the electron interaction.⁸⁻¹⁰ This explains the popularity of the Dirac-Coulomb operator in relativistic *ab initio* quantum chemistry, an operator with a relativistic one-electron part, but which treats the electron interaction at a nonrelativistic level.

The density functional counterpart of such a treatment of relativity is the Dirac-Slater model,¹¹ or variants thereof, which use more up-to-date exchange-correlation density functionals (for a recent development, see ref. 12). The name "Dirac-Kohn-Sham scheme" thus seems more appropriate. Such calculations can be viewed as a reference for more approximate relativistic treatments. They are often advertised as "fully relativistic," although they practically ignore all results from relativistic density functional theory in its proper sense,¹³⁻¹⁶ a theory mainly concerned with relativistic corrections to the electron-electron interaction.

The Dirac–Kohn–Sham reference wave function is a Slater determinant built from four-component molecular orbitals (four spinors), ψ_i :

$$\psi_i = \begin{pmatrix} \phi_i \\ \chi_i \end{pmatrix} = \begin{pmatrix} \phi_{i\alpha} \\ \phi_{i\beta} \\ \chi_{i\alpha} \\ \chi_{i\beta} \end{pmatrix} \quad (1)$$

which consist of an “upper” or “large” component, ϕ_i , and a “lower” or “small” component, χ_i . Roughly speaking, the upper and lower components are dominant in the electronic and positronic states, respectively. Both ϕ_i and χ_i are two-component functions, these two components being associated with the spin projection. The one-electron energy is given by the expectation value of the Dirac–Kohn–Sham–Slater determinant with the Dirac operator, whereas the electron interaction (electrostatic Coulomb energy and exchange-correlation energy) is evaluated from the charge density in the same way as in nonrelativistic calculations. A problem arises if one uses spin-dependent exchange-correlation functionals, which one generally wants to do in open-shell calculations. In nonrelativistic calculations, one can always choose the orbitals such that they are eigenfunctions of the z -component of the spin operator. Then, the local spin magnetization, $\vec{m}(\vec{r})$, is parallel to the z -axis everywhere and its length is simply the difference between the α and β spin densities. In relativistic calculations, this is not the case due to spin-orbit coupling. The length as well as the direction of $\vec{m}(\vec{r})$ varies (“noncollinearity”), and the notion of “spin-up” or “spin-down” is only meaningful with respect to a *local* quantization axis. The nonrelativistic exchange-correlation functionals therefore cannot be written in terms of the spin densities, but must be reformulated in terms of total density, $\rho(\vec{r})$, and the length of $\vec{m}(\vec{r})$:

$$\begin{aligned} \rho(\vec{r}) &= \sum_i \psi_i^* \psi_i \\ &= \sum_i (\phi_{i\alpha}^* \phi_{i\alpha} + \phi_{i\beta}^* \phi_{i\beta} + \chi_{i\alpha}^* \chi_{i\alpha} + \chi_{i\beta}^* \chi_{i\beta}) \end{aligned} \quad (2)$$

$$\vec{m}(\vec{r}) = \sum_i \psi_i^* \begin{pmatrix} \vec{\sigma} & 0 \\ 0 & \vec{\sigma} \end{pmatrix} \psi_i \quad (3)$$

with $\vec{\sigma}$ the vector of the Pauli spin matrices. The exchange-correlation energy is then invariant with respect to rotations in spin space. This should be

expected from a nonrelativistic functional. The procedure leads to a spin-dependent exchange-correlation potential that is a spinor potential (2×2 matrix) in the general case. For more details, the reader is referred to section IV of ref. 14. The implications of this formalism are not always fully appreciated; for example, ref. 17. A different treatment of open-shell systems in relativistic density functional theory is known as “moment polarization.”¹⁸

A survey of the literature reveals that many relativistic density functional calculations performed today are not “fully relativistic” (i.e., four-component). There are various ways^{19,20} to arrive at two-component computational schemes that contain the upper component only, all of which aim to approximate “fully relativistic” results for the electronic states. The popularity of the two-component schemes is usually explained by their lower computational cost,⁴ but in view of the large computational power available today this is not the only reason. The present investigator believes that, for applications relevant to chemistry, there is usually no *need* for fully relativistic calculations—what one really loses going from a four-component to a two-component scheme is the possibility to describe electrons and positrons simultaneously. In chemistry, we are usually only interested in electrons, and the absence of the positronic states is not a loss, but is rather convenient. However, constructing two-component Hamiltonians in which the positronic states are projected out fully satisfactorily is not at all straightforward, and some methods introduce severe problems in doing so.

Often one goes one step further and decomposes relativistic effects into a “scalar” or “spin-free” part and a spin-dependent “spin-orbit” contribution. Such a decomposition is even possible at the four-component level; that is, in the Dirac equation itself.²¹ If one considers only scalar relativistic effects, the spin variable factors off and a one-component calculation similar to the nonrelativistic case results. Such calculations are particularly successful for closed-shell compounds containing heavy atoms, because there the scalar relativistic effects are usually more important than those due to spin-orbit coupling. This is no longer true if a dissociation into open-shell fragments is considered. In this case, the spin-orbit effect on the dissociation energy stems mainly from the spin-orbit splittings in the fragments.¹⁷

We now concentrate on four different one-component, scalar-relativistic, all-electron density

functional schemes that have emerged. The oldest one is the “quasirelativistic” (QR) scheme of Ziegler, Baerends, and coworkers.^{22,23} It goes beyond leading order relativistic corrections by using the Pauli operator self-consistently. This is theoretically not well founded, because the Pauli operator is not bounded from below, and nonphysical low energies (or even divergence, if the orbitals have enough flexibility) may result from a variational treatment. The QR scheme seems to be most convenient in connection with the frozen-core approximation, where one can get a large fraction of the relativistic change of the electron density from atomic calculations. Because the QR energy expression is then made stationary with respect to variations of the valence orbitals only, the fact that the spectrum of the Pauli operator is not bounded from below might be less problematic. Rösch et al. implemented a relativistic density functional program using the Douglas–Kroll–Hess (DK) approach.^{24,25} In its one-electron approximation, one only has to modify the matrix elements of the (nonrelativistic) one-electron Hamiltonian and then proceed as in the nonrelativistic case. The matrix elements that one needs, however, cannot be evaluated in closed form. They would be easy if the basis functions were eigenfunctions of the kinetic energy operator, so one assumes completeness of the one-particle (Gaussian) basis set, diagonalizes the matrix representation of the kinetic energy operator, and evaluates the matrix elements as if the eigenvectors represented the true eigenfunctions. This approximation has consequences for the implementation of the geometry gradient (see later). Among the applications of the DK method one must mention calculations on large (highly symmetric) metal clusters with more than 100 gold²⁶ and palladium²⁷ atoms. Van Lenthe and coworkers investigated a new perturbational expansion of the Dirac equation and called this method “regular approximation.”^{28,29} To the zeroth order (ZORA), one does not obtain the (nonrelativistic) Schrödinger equation, but rather the so-called CPD equation named after Chang, Pélishier, and Durand,³⁰ who derived it via another route some time ago. ZORA and CPD are thus two different acronyms for the same method. Some noteworthy results for bond lengths, vibrational frequencies, and dissociation energies of diatomic molecules were obtained, and applications to adsorption on surfaces³¹ and magnetic properties^{32,33} were presented as well. This method has merits, but there are also severe deficiencies: In the

many-electron case, ZORA does not fulfill a stationarity condition and the direct determination of energy differences is not possible. A solution for these difficulties has very recently been proposed by the present investigator³⁴ and involves the use of a model potential to construct the ZORA kinetic energy operator (see next section). Finally, a relativistic density functional method that is a first-order perturbative scheme based on direct perturbation theory (DPT) should also be mentioned. This approach was presented together with a formalism to compute gradients.³⁵ Applications to polyatomic molecules appeared soon thereafter,^{36,37} and can also be found later in this article.

First-order DPT accounts for relativistic effects through the leading order in a consistent way. ZORA, on the other hand, is not even correct through the leading order but contains the most important higher order terms. The DK approach is based on a different expansion but is known to account for higher order relativistic effects. The QR method truncates the Pauli Hamiltonian after the leading relativistic contribution. Some higher order effects enter the QR calculation by using this first-order relativistic operator self-consistently. In principle, one could investigate the importance of higher order relativistic effects by comparing leading-order DPT data to results from one of the other calculations. In practice, however, the use of different basis sets, numerical strategies, and overall numerical accuracy makes such a comparison difficult. The DPT and ZORA results reported in this work were obtained with the same program, using equivalent basis sets and the same numerical procedures. We will therefore identify the differences between the DPT and ZORA results as higher order relativistic effects.

At the end of this section, we consider what must be done if spin-orbit effects become important. The ZORA approach has already been applied within two-component formalism¹⁷ and, for the DK method, it is clear how to proceed.²⁴ Results of the two-component DK method with full support for the (relativistic) double group symmetry have been presented very recently.³⁸ In two-component DK or ZORA calculations, spin-orbit coupling can be treated self-consistently, such that one has different radial extensions of, say, $6p_{3/2}$ and $6p_{1/2}$ spinors (orbitals) from the outset. The situation is less favorable for the QR and DPT approaches: In the QR approach, using the spin-orbit part of the Pauli operator self-consistently

probably introduces additional singularities and, in the DPT approach for open-shell systems, one must go to (quasi-)degenerate perturbation theory, which is much more complicated than the nondegenerate case. Spin-orbit effects in closed-shell molecules are higher order relativistic effects that are not contained in leading order DPT anyway.

Analytical Geometry Gradients

Quantum-chemical calculations on polyatomic molecules and chemical reactions are, in many cases, only possible if an analytical geometry gradient is available. Because relativistic effects on molecular structures (e.g., bond lengths) can be substantial, it is not possible to optimize geometries at a nonrelativistic level and use relativistic corrections only when calculating energy differences. Analytical geometry gradients are essential for automatic geometry optimizations. Some molecules with high symmetry, such as octahedral $\text{W}(\text{CO})_6$, can certainly be optimized “by hand,” but as soon as one is interested in the first tungsten–carbonyl bond dissociation energy, one must optimize the $\text{W}(\text{CO})_5$ fragment, which is already difficult to do without gradients. It was a serious drawback of earlier work (see, e.g., ref. 39) that the geometrical relaxation of the pentacarbonyl fragment could not be taken care of. This situation improved when, nearly simultaneously, analytical geometry gradients were implemented for all four relativistic density functional methods mentioned in the last section: Schreckenbach, Li, and Ziegler presented gradients for the QR scheme in 1995.⁴⁰ The formulas for this gradient are relatively simple because one can exploit the fact that self-consistent solutions for the quasirelativistic Hamiltonian have already been obtained. This is different for the DPT gradient, which was presented in the same year³⁶: In the DPT method, the relativistic correction to the total energy is computed from the nonrelativistic Kohn–Sham orbitals and their orbital energies. These orbitals optimize the nonrelativistic, but not the relativistic, energy expression. This is similar to second-order Møller–Plesset (MP2) theory, in which one derives the correlation energy from the Hartree–Fock orbitals. It is therefore no surprise that the DPT gradient involves techniques known from MP2 or CI gradients, namely the solution of a coupled Kohn–Sham system of equations to obtain a Z-vector. In 1996, Nasluzow and Rösch⁴¹ de-

scribed gradients for the (one-component) DK method. Because a DK calculation is formally no different from the nonrelativistic case, the gradient should be quite simple, the new contribution involving only geometrical derivatives of the DK matrix elements. However, these turned out to be rather complicated because of the way they were approximated: for example, one has to determine how the eigenvectors of the matrix representation of the kinetic energy operator change if basis functions move with the nuclei. In the context of *ab initio* DK theory, it has recently been proposed to evaluate the DK matrix elements using a one-center expansion.⁴² This approximation is completely geometry-independent and will thus facilitate DK gradients considerably. This “trick” should be tested in density functional DK calculations as well. Gradients for ZORA have very recently been implemented by the present investigator. This became possible after a modification of the ZORA method that makes the energy stationary with respect to orbital variations and allows direct computation of energy differences.³⁴ One-component ZORA calculations can then be done with a nonrelativistic code once the matrix elements of the one-electron Hamiltonian (or rather, its kinetic energy part) have been updated. Briefly, one adds a correction to the one-electron matrix elements, $h_{\mu\nu}$, between basis functions, B_μ and B_ν :

$$h_{\mu\nu} \rightarrow h_{\mu\nu} + \langle \vec{\nabla} B_\mu | \frac{\tilde{V}(\vec{r})}{4c^2 - 2\tilde{V}(\vec{r})} | \vec{\nabla} B_\nu \rangle \quad (4)$$

with $\tilde{V}(\vec{r})$ a model potential that depends on the molecular geometry only and c the velocity of light, which is ~ 137 a.u. These matrix elements must be evaluated using numerical quadrature, and special grids (“ZORA grids”) have been designed for this task that are somewhat larger than the grids used in the Kohn–Sham iterations. This is not harmful because this integration needs to be done only once in a calculation, not in each SCF cycle.

The model potential consists of a nuclear part and Coulomb- and exchange-correlation contributions that are derived from model density, $\tilde{\rho}(\vec{r})$:

$$\tilde{V}(\vec{r}) = - \sum_A \frac{Z_A}{|\vec{r} - \vec{R}_A|} + \int \frac{\tilde{\rho}(\vec{\tau})}{|\vec{r} - \vec{\tau}|} d\vec{\tau} + \frac{\delta F_{xc}}{\delta \tilde{\rho}} \quad (5)$$

where the sum runs over the atoms A with nuclear charge Z_A located at position \vec{R}_A , and the

exchange-correlation potential is derived from an exchange-correlation functional F_{xc} . For the model density, one uses a sum of spherical atomic model densities (note that a sum of atomic model potential cannot be used—see ref. 34), which are expanded in a Gaussian basis:

$$\tilde{\rho}(\vec{r}) = \sum_A \tilde{\rho}_A(|\vec{r} - \vec{R}_A|) \quad (6)$$

$$\tilde{\rho}_A(r) = \sum_i c_{iA} \exp(-\alpha_{iA} r^2) \quad (7)$$

and where the (fixed) parameters c_{iA} and α_{iA} have been determined from a fit of $\tilde{\rho}_A$ to densities obtained in atomic calculations. After the one-electron matrix elements have been updated, the calculation proceeds exactly as in the nonrelativistic case. Relativity is thus treated self-consistently and the gradient can therefore be evaluated using the nonrelativistic code, except for one additional contribution, which involves geometrical derivatives of the matrix element eq. (4). From nonrelativistic theory, we know how to evaluate such derivatives once we can calculate, at a given grid point, \vec{r}_j , the derivatives of the model potential, $\tilde{V}(\vec{r}_j)$, with respect to nuclear displacements. The evaluation of these derivatives is straightforward³⁴ from eqs. (5)–(7). The derivative of the matrix element [eq. (4)] must be evaluated using the “ZORA grid.” When passing through this grid in the gradient calculation, all other density functional gradient contributions can be evaluated on the fly with little extra cost. Therefore, it was decided to use the larger (and more accurate) grid for all gradient contributions. Note that the ZORA gradient is less expensive than the DPT gradient, because one must solve a coupled Kohn–Sham equation in the latter case. In fact, a ZORA geometry optimization is not more expensive than a nonrelativistic calculation, whereas $\sim 50\%$ more CPU time is needed for a DPT geometry optimization.

Metal–Carbon Bond Length and First Metal–Carbonyl Bond Dissociation Energy for Some Transition Metal Carbonyls: Comparison of Various Relativistic Methods

In this section we compare results obtained with the four relativistic density functional methods just described. We compare only calculations that

use the same exchange-correlation functional, namely an exchange functional due to Becke⁴³ and a correlation functional due to Perdew.⁴⁴ All calculations in the present work use this functional. The metal basis sets used in the DPT and ZORA calculations are described in the Appendix, and triple-zeta-type basis sets with a set of polarization functions have been used for the ligand atoms C and O. All binding energies obtained in the present work have been corrected for the basis-set superposition effect (BSSE). QR and DK results were taken from the literature.^{40,41,45} The data for molybdenum and tungsten hexacarbonyl, ruthenium and osmium pentacarbonyl, and palladium and platinum tetracarbonyl can be found in Table I. These molecules are benchmark compounds for which much computational and experimental data are available. It is not necessary to comment upon these data in detail because this has already been done elsewhere. With few exceptions, the calculations agree with each other and with experiment. Note that the experimental bond dissociation energy may be incorrect for $\text{Os}(\text{CO})_5$, because it comes from kinetic experiments where the assumed reaction mechanism might be wrong.⁴⁶ For $\text{Os}(\text{CO})_5$ and $\text{Pt}(\text{CO})_4$, the QR bond lengths are significantly longer than for the other calculations. This is probably not caused by the treatment of relativity, because such a discrepancy occurs already at the nonrelativistic level.³⁶ In this context, it should be noted that, in a more recent study,⁴⁷ slightly different QR results have been reported for $\text{Mo}(\text{CO})_6$ (Mo–C: 207.0 pmol, D_e : 167 kJ/mol) and $\text{W}(\text{CO})_6$ (W–C: 206.6 pmol, D_e : 193 kJ/mol), which show better agreement with the other computational results. Most noteworthy is the agreement between the DPT and ZORA results. For the second-row transition metal carbonyls, the differences in bond lengths between DPT and ZORA are much less than 1 pmol, and the difference is ~ 1 pmol for the third-row carbonyls. For the latter compounds, the ZORA bond dissociation energies are slightly less when compared with the DPT results. This is unexpected, because higher order relativistic effects, if they play a role, should further increase the binding energy. It can be summarized that higher order relativistic effects play only a minor role, even for the third-row transition metal compounds studied here. The situation is different for gold and eka-gold (element 111) compounds,^{34,48} where differences between ZORA and DPT are much larger.

TABLE I.
Metal–Carbon Bond Lengths and First CO Dissociation Energies of Some Transition Metal Carbonyls.

	DPT ^a	ZORA ^a	DK ^b	QR ^c	Exp. ^d
Mo(CO) ₆					
Mo—C [pm]	206.7	206.5	206.8	207.6	206.3
D _e [kJ mol ^{−1}]	161	161	165	166	170 ± 8
Ru(CO) ₅					
Ru—C _{ax} [pm]	195.8	195.6		196.8	195.0
Ru—C _{eq} [pm]	196.0	195.7		196.0	196.9
D _e [kJ mol ^{−1}]	132	132		138	116
Pd(CO) ₄					
Pd—C [pm]	201.0	200.6		205.6	
D _e [kJ mol ^{−1}]	52	52		51	
W(CO) ₆					
W—C [pm]	206.0	205.2	206.3	204.9	205.8
D _e [kJ mol ^{−1}]	190	189	196	183	193 ± 8
Os(CO) ₅					
Os—C _{ax} [pm]	196.6	195.8		200.0	199.0
Os—C _{eq} [pm]	195.1	194.0		197.5	194.3
D _e [kJ mol ^{−1}]	161	157		145	128
Pt(CO) ₄					
Pt—C [pm]	196.9	195.3		201.2	
D _e [kJ mol ^{−1}]	66	62		66	

^a DPT and ZORA, present work. ^b Douglas–Kroll DFT calculation, ref. 41. ^c Quasi-relativistic method, refs. 40 and 45. ^d Refs. 46, 64–68.

Metal–Phosphine Bond in Tungsten and Platinum Carbonyl Phosphine Complexes and Stability of Mixed Dinitrogen Phosphine Molybdenum Carbonyls

Some demonstrative applications of the DPT density functional method are now presented. The compounds W(CO)₅L and Pt(CO)₃L have been studied for a variety of phosphine ligands, L, namely PH₃, PMe₃, P(ⁱC₃H₇)₃, PF₃, PCl₃, PBr₃, and P(CF₃)₃, to elucidate the contributions of both σ basicity and π acidity to the trends in the metal–phosphorus binding energy. In principle, such a study can be based on the analysis of the wave function; that is, a population analysis or a variant thereof, the so-called “charge decomposition analysis” (CDA), which was introduced by Dapprich and Frenking⁴⁹ and used subsequently for the analysis of backbonding in carbonyl compounds.⁵⁰ In this work we proceed differently and base the analysis on observable properties of the molecule, such as binding energies, bond lengths, and force constants. Such an approach is more directly connected to experimental strategies.^{51–55}

Basically, if ligand L is a good π -acceptor, it will reduce the backbonding to the carbonyls. This makes the metal–carbon bond weaker and the carbon–oxygen bond stronger. In the case of the octahedral tungsten complexes, this effect is larger for the trans (axial) carbonyl ligand than for the four equatorial CO groups. If ligand L is a good σ -donor, this will enhance backbonding to the carbonyls, but this effect is not much different for the cis and trans carbonyls. Table II shows tungsten–phosphorus and axial tungsten–carbon bond lengths and binding energies (BSSE-corrected) as well as force constants of the symmetric cis (k_{cis}) and the trans (k_{tr}) CO stretching modes. The force constants have been obtained by numerical differentiation of analytical geometry gradients. For comparison, results are also given for the ligands NMe₃ (which is a σ -donor, but has no π acidity), N₂ (which acts as a π -acceptor but has low σ basicity), and CH₂ (which is a σ -donor but also a very good π -acceptor). All these calculations used double-zeta-type basis sets (with a set of polarization functions) for the ligand atoms. For convenience and to facilitate the analysis, k_{cis} has been divided by four, because four CO ligands stretch

TABLE II.
Calculated Bond Lengths, Bond Dissociation Energies, and C=O Force Constants in Octahedral W(CO)₅L Complexes.

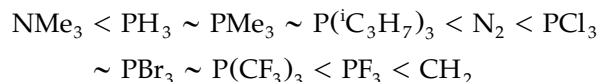
L	W—P ^a	W—C _{ax} ^b	D _e (W—P) ^c	D _e (W—C _{ax}) ^c	k _{cis} ^d	k _{tr} ^e
PH ₃	251.8	201.5	138	233	1650	1593
PMe ₃	254.2	202.0	182	227	1629	1584
P(ⁱ C ₃ H ₇) ₃	260.7	201.0	148	234	1618	1575
PF ₃	239.9	202.9	147	205	1683	1638
PCl ₃	244.2	202.7	122	209	1681	1629
PBr ₃	245.7	202.6	107	210	1677	1620
P(CF ₃) ₃	245.2	202.7	121	214	1673	1622
NMe ₃		199.1		265	1626	1559
N ₂		202.2		233	1678	1605
CH ₂		210.0		159	1678	1645

^a Tungsten–phosphorus bond length in pm. ^b Axial tungsten–carbon bond length in pm. ^c Bond dissociation energy in kJ mol^{−1}.^d Diagonal force constant of symmetric *cis*-CO stretching mode in N m^{−1}, divided by four. ^e Diagonal force constant of *trans*-CO stretching mode in N m^{−1}.

simultaneously. In the nomenclature of Kraihanzel and Cotton,⁵¹ k_{tr} corresponds to their k_1 value, whereas k_{cis} is equal to $k_2 + 4k_i$.

The tungsten–phosphorus bond length shows considerable variation, ranging from 240 pm for the trifluorophosphine ligand to 260 pm in the case of triisopropylphosphine. In the latter case, the long bond can be explained with steric repulsion, which is also responsible for the low bond dissociation energy of only 148 kJ/mol—compared with the value for trimethylphosphine, which amounts to 182 kJ/mol. For the electronegative phosphines [PF₃, PCl₃, PBr₃, and P(CF₃)₃] one finds both rather short metal–phosphorus bond lengths and low dissociation energies. This trend is uncommon in chemistry, where shorter bonds are usually associated with higher dissociation energies. Because the axial metal–carbon bond lengths are rather long (and their dissociation energy rather low) for the electronegative phosphines, one can assume that these phosphines act as π -acceptors. The low metal–phosphorus bond energy must therefore come from the low σ basicity of these phosphines. For PF₃, the axial W—C bond is the longest, its dissociation energy the lowest, and the axial CO force constant (k_{tr}) the highest of all phosphines studied. The data show that there is considerable π acidity for PF₃. The short metal–phosphorus bond lengths for PF₃ and similar phosphines is related to their low σ basicity; that is, the higher s-character of the P lone pair forming the metal–phosphorus σ bond. This follows from a general rule.⁵⁶ Comparing both *trans* (k_{tr}) and *cis* (k_{cis}) CO force constants, one can

distinguish between σ and π effects; that is, going from PH₃ to PMe₃, k_{cis} changes by 21 N/m, but k_{tr} only by 11 N/m. This means that PMe₃ differs from PH₃ primarily because it is a better σ -donor. Going from PF₃ to P(CF₃)₃, on the other hand, has a smaller effect on k_{cis} (10 N/m) than on k_{tr} (16 N/m). This means that the main difference between these two ligands is that PF₃ is the better π -acceptor. The differences between the trimethyl- and triisopropylphosphine complexes probably do not come from different electronic properties of the free ligands, but from the fact that the metal–phosphorus bond length is much larger in the latter case (for steric reasons), so the overlap is automatically lower and reduces both σ basicity and π acidity. The axial tungsten–carbonyl dissociation energy is large (more backbonding to the carbonyl) if ligand L is a weak π -acceptor. This correlation has been studied in ref. 37. The data obtained for the axial carbonyl ligand (metal–carbon bond length, metal–carbonyl dissociation energy, carbonyl stretching force constant) show that π acidity increases in the order:



For the platinum tricarbonyl phosphines (Table III), similar results were obtained. Because the three carbonyl ligands are equivalent, one cannot distinguish between σ and π effects as in the case of the tungsten complexes. So, we give the symmetric CO and Pt—C stretching force constants

TABLE III.
Calculated Bond Lengths, Bond Dissociation Energies, and Symmetric C=O and Pt—C Stretch Force Constants in Tetrahedral Pt(CO)₃L Complexes.

L	Pt—P ^a	Pt—C ^b	D _e (Pt—P) ^c	k _{C—O} ^d	k _{Pt—C} ^e
PH ₃	241.5	194.6	45	1660	314
PMe ₃	240.6	194.1	80	1631	322
PF ₃	228.7	195.9	47	1701	292
PCl ₃	236.9	195.5	31	1696	299
PBr ₃	239.8	195.4	30	1696	300
P(CF ₃) ₃	233.0	195.5	39	1689	298

^a Platinum—phosphorus bond length in pm.

^b Platinum—carbon bond length in pm. ^c Bond dissociation energy in kJ mol⁻¹. ^d Symmetric CO stretch force constant in N m⁻¹, divided by 3. ^e Symmetric Pt—C stretch force constant in N m⁻¹, divided by 3.

and find the expected correlation: high CO force constants (little backbonding from Pt to CO) correspond to low Pt—C bond strengths and long Pt—C bonds. Note that the platinum—phosphorus binding energies are much lower than the values obtained for the tungsten compounds.

The results suggest that two ligands, L₁ and L₂, where L₁ is a weak π -acceptor but a strong σ -donors, and the opposite holds for L₂, can stabilize each other if bound to the same metal atom, especially if they occupy trans positions in an octahedral complex. This was confirmed by calculations performed for Mo(CO)₅(N₂), Mo(CO)₅(PX₃) and *trans*-Mo(CO)₄(N₂)(PX₃) for X=H and X=F (Table IV). If the ligand trans to dinitrogen changes from CO to PH₃, the Mo—N bond length decreases from 213 to 208 pm, and its dissociation energy increases from 83 to 103 kJ/mol. PF₃ is somewhere between PH₃ and CO but closer to the latter: substituting a trans CO group with PF₃ increases the Mo—N binding energy by only 4 kJ/mol. The molybdenum—phosphine bond also becomes stronger if it is trans to dinitrogen: in *trans*-

Mo(CO)₄(N₂)(PH₃), both the Mo—N and Mo—P bond dissociation energies are higher than in molybdenum dinitrogen pentacarbonyl or molybdenum pentacarbonyl phosphine, respectively.

Metal–Fluorine Stretching Force Field for Molybdenum, Tungsten, and Uranium Hexafluoride

In the previous section, some force constants were discussed. In this study, these force constants were obtained from a numerical differentiation of analytical geometry gradients. While this procedure is much more accurate and efficient than obtaining force constants from numerical second derivatives of total energy, it is competitive (at least in terms of efficiency) with analytical second derivatives, which have not been implemented so far. This section presents DPT and ZORA results for the equilibrium geometry and parts of the force field of octahedral MF₆ complexes (M=Mo, W, U). Considering only metal–fluorine stretching modes, there are three force constants: the diagonal M—F stretching force constant f_r and the off-diagonal force constants f_{rr} and $f_{rr'}$ of two M—F bonds in cis or trans positions, respectively. The force constant for the totally symmetric mode, which determines the highest vibrational frequency, $\nu_{a_{1g}}$ of the molecule, is then given by:

$$F_{11} = 6(f_r + 4f_{rr} + f_{rr'}) \quad (8)$$

Independent from eq. (8), F_{11} has also been obtained directly from totally symmetric geometry variations of the molecule, and no discrepancy has been found. The results are compiled in Table V, together with experimental values and data from quasirelativistic X_α calculations. Experimentally, it is much easier to extract $f_r + f_{rr'}$ than both constants individually from the spectrum and, for

TABLE IV.
Molecular Structure and Binding Energies of Molybdenum Dinitrogen Phosphine Carbonyls.

	R(Mo—P) [pm]	R(Mo—N) [pm]	D _e (Mo—P) [kJ mol ⁻¹]	D _e (Mo—N) [kJ mol ⁻¹]
Mo(CO) ₅ (N ₂)		212.8		83
Mo(CO) ₅ (PH ₃)	252.7		116	
Mo(CO) ₅ (PF ₃)	240.3		120	
<i>trans</i> -Mo(CO) ₄ (N ₂)(PH ₃)	248.0	207.9	139	103
<i>trans</i> -Mo(CO) ₄ (N ₂)(PF ₃)	235.3	210.8	146	87

TABLE V.
Bond Lengths and Metal—Fluorine Stretch
Force Field of Molybdenum, Tungsten, and
Uranium Hexafluoride.

	DPT ^a	ZORA ^a	QRX _α ^b	Exp. ^c
MoF ₆				
Mo—F [pm]	186.8	186.8	185	182.0
<i>f_r</i> [N m ^{−1}]	412	410		485
<i>f_{rr}</i> [N m ^{−1}]	16	16		25
<i>f_{rr'}</i> [N m ^{−1}]	30	30		
<i>ν_{α_{1g}}</i> [cm ^{−1}]	674	673	690	741
WF ₆				
W—F [pm]	185.6	185.5	189	183.2
<i>f_r</i> [N m ^{−1}]	469	466		550
<i>f_{rr}</i> [N m ^{−1}]	19	20		27
<i>f_{rr'}</i> [N m ^{−1}]	39	39		42
<i>ν_{α_{1g}}</i> [cm ^{−1}]	723	723	791	720
UF ₆				
U—F [pm]	205.2	202.5	205	199.9
<i>f_r</i> [N m ^{−1}]	333	338		385
<i>f_{rr}</i> [N m ^{−1}]	20	22		30
<i>f_{rr'}</i> [N m ^{−1}]	6	6		1
<i>ν_{α_{1g}}</i> [cm ^{−1}]	610	624	660	672

^a Present work. ^b Quasirelativistic X_α, ref. 57. ^c MoF₆: force field derived from observed frequencies (ref. 69) and using the value for *f_{rr'}*, calculated in the present work; WF₆: force field derived from harmonic frequencies, ref. 70; UF₆: force field derived from harmonic frequencies (ref. 71), bond lengths from refs. 72 and 73.

MoF₆, it seems that only this sum is known accurately. The “experimental” Mo—F stretching constant, *f_r*, has therefore been computed using the value of *f_{rr'}* obtained in the present calculation. If we compare the DPT and ZORA results, we find complete agreement for MoF₆ and WF₆. This had to be expected from the results on the carbonyls presented earlier: leading-order relativistic perturbation theory seems to be sufficient in these cases. Larger differences between DPT and ZORA occur for the uranium compound: the ZORA bond length is nearly 3 pm shorter, and the ZORA force constants are somewhat larger. For all three compounds, the bond lengths are larger than the experimental values, and the force constants are smaller. This trend has also been observed in a series of *ab initio* (MP2) and various density functional calculations on WF₆ using quasirelativistic pseudopotentials.⁵⁷ As a result of the present work, one can exclude that this was an artifact of the pseudopotential, as has been speculated. Note that the force field of uranium hexafluoride is qualita-

tively different from that of the group 6 metals: for molybdenum and tungsten hexafluoride, the force constant *f_{rr'}* (coupling of two M—F bonds trans to each other) is quite large, in fact twice as large as *f_{rr}* (coupling of two cis M—F stretches). This trans effect (which follows from symmetry properties of the metal d orbitals) has already been mentioned in this article. For the uranium compound, *f_{rr}* is much *larger* than *f_{rr'}*, so there is a distinct difference between uranium on one side and the group 6 metals on the other. The fact that, for the value of *f_{rr'}*, there is a disagreement between the calculations (6 N/m) and experiment (1 N/m) does not invalidate this conclusion. Note that *f_{rr'}* is difficult to determine experimentally.

Conclusions and Outlook

Relativistic density functional methods have advanced significantly during recent years. Within a short period of time, analytical geometry gradients for several relativistic one-component all-electron density functional methods have been developed. This extends the applicability of relativistic density functional theory considerably. In the future, gradients will probably also be available for two-component variants of these methods, including spin-orbit effects. The Douglas–Kroll and ZORA approaches are most promising in this respect. Gradients for the “fully relativistic” four-component Dirac–Kohn–Sham method are also being developed,⁵⁸ but could not yet be reviewed here. Most probably, four-component methods are not needed for applications such as geometry optimizations, evaluations of binding energies, etc. Douglas–Kroll and ZORA approaches have the advantage that they include, self-consistently, higher orders of relativistic (including spin-orbit) effects. For both methods (in the one-component variant), the calculation proceeds exactly as in the nonrelativistic case once the matrix elements of the one-particle Hamiltonian have been updated. This greatly simplifies the implementation of analytical geometry gradients and makes these calculations no more expensive than their nonrelativistic counterpart. I speculate that these two methods will survive over the long term. The DPT and QR methods are widely used today but have drawbacks: the QR method is weakly founded from a purely theoretical point of view, to the extent that higher order relativistic corrections are concerned. DPT calculations underestimate relativistic effects

if they are very large (as for gold and uranium compounds), and an extension of the DPT method to higher orders as well as quasidegenerate DPT for open-shell situations exist, but are rather complicated.

Appendix: Basis Sets and Integration Grids

Large basis sets have been used for some metal atoms. For Mo, Ru and Pd, a 23s16p13d primitive basis set was taken from ref. 59 and augmented by one p-function with the next exponent of the well-tempered series. These basis sets were contracted to 17s12p10d. For W, Os, and Pt, a 24s17p15d10f basis set from the same source was augmented by one p-function and contracted to 18s13p11d7f. For uranium, a 26s21p17d12f primitive basis set from ref. 60 was contracted to 20s16p13d9f. Double- and triple-zeta-type basis sets for the ligand atoms were taken from ref. 61. For ZORA, new contraction coefficients were obtained based on atomic ZORA calculations. This was necessary because here one calculates relativistic orbitals, whereas the DPT energy was evaluated from the nonrelativistic wave functions.

Accurate numerical integration grids were used. To evaluate the exchange-correlation energy and the matrix elements of the exchange-correlation potential, 10,662 grid points were used for each H atom; 21,656 points for C, N, O, and F; 23,690 points for P; 28,446 points for Mo, Ru, and Pd; 30,784 points for W, Os, and Pt; and 32,686 points for the uranium atom. To integrate the ZORA matrix elements [eq. (4)], the grid needed to be somewhat larger (see ref. 34 for details): 23,216 points for C, O, and F; 59,848 points for Mo, Ru, and Pd; 65,812 points for W, Os, and Pt; and 111,684 points for the uranium atom.

The radial parts of the integration grid follow the recommendation of Treutler and Ahlrichs.⁶² The angular resolution in each radial shell decreases going from the valence to the core region. However, for atoms with f-functions in the basis set, even the innermost radial shell must have an angular grid that is exact up to at least $l = 6$. Otherwise, large errors occur when integrating *matrix elements* of the exchange-correlation potential, eventually yielding artificially deformed core densities. This important point has not always been fully appreciated; for example, in the so-called "standard grid,"⁶³ the innermost radial shells had

only six grid points exact up to $l = 3$ only. Note that fixing this problem would not affect efficiency: Because most grid points are in the valence region anyway, increasing the number of angular grid points in the core region to a reasonable value (e.g., 38 points, $l = 9$) would have only a small effect on the size of the integration grid.

References

1. Dirac, P. A. M. *Proc Soc. London A* 1929, 123, 714.
2. Primas, H. *Chemistry, Quantum Mechanics and Reductionism* (Lecture Notes in Chemistry, Vol. 24); Springer: Berlin, 1981.
3. Pyykkö, P. *Chem Rev* 1988, 88, 563.
4. Hess, B. A. *Ber Bunsenges Physik Chem* 1997, 101, 1.
5. Jonas, V.; Thiel, W. *J Chem Phys* 1995, 102, 8474.
6. Breit, G. *Phys Rev* 1929, 34, 553.
7. Pyykkö, P.; Tokman, M.; Labzowsky, L. N. *Phys Rev A* 1998, 57, R689.
8. Visscher, L.; Dyall, K. G. *J Chem Phys* 1996, 104, 9040.
9. Mayer, M.; Häberlen, O. D.; Rösch, N. *Phys Rev A* 1996, 54, 4775.
10. Liu, W.; Küchle, W.; Dolg, M. *Phys Rev A* 1998, 58, 1103.
11. Rosen, A.; Ellis, D. E. *J Chem Phys* 1975, 62, 3039.
12. Liu, W.; Hong, G. Y.; Dai, D. D.; Li, L. M.; Dolg, M. *Theor Chem Acc* 1997, 96, 75.
13. McDonald, A. H.; Voski, S. H. *J Phys C* 1979, 12, 2977.
14. Ramana, M. V.; Rajagopal, A. K. *Adv Chem Phys* 1983, 54, 231.
15. Engel, E. *Int J Quantum Chem* 1995, 56, 217.
16. Engel, E.; Keller, S.; Bonetti, A. F.; Müller, H.; Dreizler, R. M. *Phys Rev A* 1995, 52, 2750.
17. van Lenthe, E.; Snijders, J. G.; Baerends, E. J. *J Chem Phys* 1996, 105, 6505.
18. Ellis, D. L.; Goodman, G. L. *Int J Quantum Chem* 1984, 25, 185.
19. Kutzelnigg, W. *Z Phys D* 1990, 15, 27.
20. Kutzelnigg, W. *Chem Phys* 1997, 225, 203.
21. Dyall, K. G. *J Chem Phys* 1994, 100, 2118.
22. Ziegler, T.; Snijders, J. G.; Baerends, E. J. *J Chem Phys* 1981, 74, 1271.
23. Ziegler, T.; Tschinke, V.; Baerends, E. J.; Snijders, J. G.; Ravenek, W. *J Phys Chem* 1989, 93, 3050.
24. Knappe, P.; Rösch, N. *J Chem Phys* 1990, 92, 1153.
25. Häberlen, O. D.; Rösch, N. *Chem Phys Lett* 1992, 199, 491.
26. Häberlen, O. D.; Chung, S. C.; Stener, M.; Rösch, N. *J Chem Phys* 1997, 106, 5189.
27. Krüger, S.; Vent, S.; Rösch, N. *Ber Bunsenges Physik Chem* 1997, 101, 1640.
28. van Lenthe, E.; Baerends, E. J.; Snijders, J. G. *J Chem Phys* 1993, 99, 4597.
29. van Lenthe, E.; Baerends, E. J.; Snijders, J. G. *J Chem Phys* 1994, 101, 9783.
30. Chang, C.; Péliissier, M.; Durand, P. *Phys Scr* 1986, 34, 394.

31. Philipsen, P. H. T.; van Lenthe, E.; Snijders, J. G.; Baerends, E. J. *Phys Rev B* 1997, 56, 13556.
32. van Lenthe, E.; Wormer, P. E. S.; van der Avoird, A. *J Chem Phys* 1997, 107, 2488.
33. van Lenthe, E.; van der Avoird, A.; Wormer, P. E. S. *J Chem Phys* 1998, 108, 4783.
34. van Wüllen, C. *J Chem Phys* 1998, 109, 392.
35. van Wüllen, C. *J Chem Phys* 1995, 103, 3589.
36. van Wüllen, C. *J Chem Phys* 1996, 105, 5485.
37. van Wüllen, C. *J Comput Chem* 1997, 18, 1985.
38. N. Rösch et al., presented at a colloquium on relativistic methods, Kassel, Germany, May 1998.
39. Ziegler, T.; Tschinke, V.; Ursenbach, C. *J Am Chem Soc* 1987, 109, 4825.
40. Schreckenbach, G.; Ziegler, T.; Li, J. *Int J Quantum Chem* 1995, 56, 477.
41. Nasluzov, V. A.; Rösch, N. *Chem Phys* 1996, 210, 413.
42. Sjøvoll, M.; Fagerli, H.; Gropen, O.; Almlöf, J.; Schim-melpfennig, B.; Wahlgren, U. *Theor Chem Acc* 1998, 99, 1.
43. Becke, A. D. *Phys Rev A* 1988, 38, 3098.
44. Perdew, J. P. *Phys Rev B* 1986, 33, 8822.
45. Li, J.; Schreckenbach, G.; Ziegler, T. *J Am Chem Soc* 1995, 117, 486.
46. Shen, J. K.; Gao, Y. C.; Shi, Q. Z.; Basolo, F. *Inorg Chem* 1989, 28, 4304.
47. Ehlers, A. W.; Ruiz-Morales, Y.; Baerends, E. J.; Ziegler, T. *Inorg Chem* 1997, 36, 5031.
48. Liu, W.; van Wüllen, C. *J Chem Phys* (in press).
49. Dapprich, S.; Frenking, G. *J Phys Chem* 1995, 99, 9352.
50. Ehlers, A. W.; Dapprich, S.; Vyboishchikov, S. F.; Frenking, G. *Organometallics* 1996, 15, 105.
51. Kraihanzel, C. S.; Cotton, F. A. *J Am Chem Soc* 1962, 84, 4432.
52. Graham, W. A. G. *Inorg Chem* 1968, 7, 315.
53. Brown, R. A.; Dobson, G. R. *Inorg Chim Acta* 1972, 6, 65.
54. Apel, J.; Grobe, J. Z. *Anorg Allg Chemie* 1979, 453, 53.
55. Davies, M. S.; Armstrong, R. S.; Aroney, M. J. *Chim Chron* 1995, 24, 233.
56. Jonas, V.; Boehme, C.; Frenking, G. *Inorg Chem* 1996, 35, 2097.
57. Parsons, I. W.; Till, S. J. *J Chem Soc Faraday Trans* 1993, 89, 25.
58. B. Fricke et al., presented at a colloquium on relativistic methods, Kassel, Germany, May 1998.
59. Huzinaga, S.; Klobukowski, M. *J Mol Struct (Theochem)* 1988, 167, 1.
60. de Jong, W. A. PhD thesis, Groningen 1998. The second s-exponent has been corrected to 13,449,948.46 (W. A. de Jong, private communication).
61. Schäfer, A.; Ahlrichs, R. *J Chem Phys* 1992, 97, 2571.
62. Treutler, O.; Ahlrichs, R. *J Chem Phys* 1995, 102, 346.
63. Gill, P. M. W.; Johnson, B. G.; Pople, J. A. *Chem Phys Lett* 1993, 209, 506.
64. Arnesen, S. P.; Seip, H. M. *Acta chem Scand* 1966, 20, 7711.
65. Juang, J.; Hedberg, K.; Davis, H. B.; Pomeroy, R. K. *Inorg Chem* 1990, 29, 3923.
66. Huang, J.; Hedberg, K.; Pomeroy, R. K. *Organometallics* 1988, 7, 2049.
67. Lewis, K. E.; Golden, D. M.; Smith, G. P. *J Am Chem Soc* 1984, 106, 3905.
68. Huq, R.; Poe, A. J.; Chalwa, S. *Inorg Chim Acta* 1980, 38, 121.
69. Kimura, M.; Kimura, K. *J Molec Spectrosc* 1963, 11, 368.
70. McDowell, R. S.; Asprey, L. B. *J Molec Spectrosc* 1973, 48, 254.
71. McDowell, R. S.; Asprey, L. B.; Paine, R. T. *J Chem Phys* 1974, 61, 3571.
72. Seip, H. M.; Seip, R. *Acta Chem Scand* 1966, 20, 2698.
73. Seip, H. M. *Acta Chem Scand* 1965, 19, 1965.